RHEUMATOLOGY

Rheumatology 2018;57:1105–1114
doi:10.1093/rheumatology/kex525
Advance Access publication 7 March 2018

Original article

Neutralization of CD40 ligand costimulation promotes bone formation and accretion of vertebral bone mass in mice

Susanne Roser-Page[1], Tatyana Vikulina[1,2], Kanglun Yu[3], Meghan E. McGee-Lawrence[3,4] and M. Neale Weitzmann[1,2,5]

Abstract

Objective. Immunosuppressive biologics are used in the management of RA and additional immunomodulators are under investigation including modulators of the CD40/CD40 ligand (CD40L) costimulation pathway. Tampering with immune function can have unanticipated skeletal consequences due to disruption of the immuno-skeletal interface, a nexus of shared cells and cytokine effectors serving discrete functions in both immune and skeletal systems. In this study, we examined the effect of MR1, a CD40L neutralizing antibody, on physiological bone remodelling in healthy mice.

Methods. Female C57BL6 mice were treated with MR1 and BMD was quantified by dual energy X-ray absorptiometry and indices of trabecular bone structure were quantified by micro-CT. Serum biochemical markers were used to evaluate bone turnover and formation indices by histomorphometry.

Results. Unexpectedly, MR1 stimulated significant accretion of BMD and trabecular bone mass in the spine, but not in long bones. Surprisingly, bone accretion was accompanied by a significant increase in bone formation, rather than suppression of bone resorption. Mechanistically, MR1-induced bone accrual was associated with increased Treg development and elevated production of cytotoxic T lymphocyte antigen 4, a costimulation inhibitor that promotes T cell anergy and $CD8^+$ T cell expression of the bone anabolic ligand Wnt-10b.

Conclusion. Our studies reveal an unexpected bone anabolic activity of pharmacological CD40L suppression. Therapeutic targeting of the CD40L pathway may indeed have unforeseen consequences for the skeleton, but may also constitute a novel strategy to promote bone formation to ameliorate osteoporotic bone loss and reduce fracture risk in the axial skeleton.

Key words: osteoblast, T cell, Wnt-10b, CD40 ligand, MR1, bone formation, rheumatoid arthritis

BASIC SCIENCE

Rheumatology key messages

- Due to the immuno-skeletal interface, pharmacological manipulation of immune functions can drive skeletal changes, including stimulation of bone anabolism.
- Pharmacological suppression of CD40 ligand signalling in healthy mice causes a bone anabolic response.
- CD40 ligand neutralization induces Tregs and cytotoxic T lymphocyte antigen 4 production leading to T cell Wnt-10b production and bone formation.

[1]Atlanta VA Medical Center, Decatur, [2]Division of Endocrinology and Metabolism and Lipids, Department of Medicine, Atlanta, [3]Department of Cellular Biology and Anatomy, [4]Department of Orthopaedic Surgery, Medical College of Georgia, Augusta University, Augusta and [5]The Winship Cancer Institute, Emory University School of Medicine, Atlanta, GA, USA

Submitted 25 May 2017; revised version accepted 13 December 2017

Correspondence to: M. Neale Weitzmann, Division of Endocrinology and Metabolism and Lipids, Emory University School of Medicine, 101 Woodruff Circle, 1305 WMB, GA 30322-0001, USA.
E-mail: mweitzm@emory.edu

Introduction

The CD40 ligand (CD40L) T cell costimulation pathway is presently under investigation as an immunomodulatory target for amelioration of inflammatory conditions such as RA [1, 2].

CD40–CD40L interactions mediate many cell-mediated immune responses and T cell-mediated effector functions that are required for proper functioning of the host defence

system [3]. Following initial T cell activation, CD40L is transiently upregulated on T cells and associates with its cognate receptor CD40 on antigen-presenting cells (APCs). This bidirectional signal sustains the immune response for as long as the antigen remains in the system and promotes effector functions of T cells as well as supporting APC function and promoting humoral immunity [1, 3, 4].

Wnt-10b is a bone anabolic factor known to be secreted by T cells following intermittent parathyroid hormone (PTH) treatment [5], as well as by T cells treated with cytotoxic T lymphocyte antigen 4 (CTLA-4) Ig, also known as abatacept. CTLA-4Ig is a pharmacological CD28 costimulation inhibitor that renders T cells anergic and unresponsive to further antigen presentation [6]. As CD40L blockade has been reported to promote T cell anergy [7] and CD40L inhibitors thus have the potential to stimulate bone formation, we investigated the effect of pharmacological CD40L suppression by MR1 antibody on physiological bone turnover, BMD and trabecular and cortical bone structure in healthy mice.

Our data reveal a significant gain of bone mass following MR1 treatment, a result of a bone anabolic response characterized by stimulation of bone formation. Increased bone formation led to the significant accretion of trabecular bone mass in the lumbar spine, but not in long bones. Mechanistically, our data suggest a putative model whereby CD40L neutralization promotes increased $CD4^+$ T cell differentiation into Tregs, a population that produces CTLA-4, which in turn promotes production of the bone anabolic ligand, Wnt-10b by $CD8^+$ T cells, stimulating bone formation.

Methods

All chemicals and reagents were purchased from the Sigma-Aldrich Chemical Co. (St Louis, MO, USA), unless otherwise indicated. All animal studies were approved by the Animal Care and Use Committees of both the Atlanta VA Medical Center and Emory University, and were conducted in accordance with the National Institutes of Health (NIH) Laboratory Guide for the Care and Use of Laboratory Animals.

Female C57BL6 mice from Charles River Laboratories International (Wilmington, MA, USA) were used in all studies and housed under specific pathogen-free conditions and fed gamma-irradiated 5V02 mouse chow (Purina Mills, St Louis, MO, USA) and autoclaved water *ad libitum*.

Skeletally mature female C57BL6 (5 months of age) mice from Charles River Laboratories International (Wilmington, MA, USA) were injected intraperitoneally monthly for 6 months with 10 mg/kg MR1 anti-CD40L antibody (Taconic Biosciences, Germantown, NY, USA) or with 10 mg/kg hamster IgG (Ig) isotype control (Lampire Biological Laboratories, Pipersville, PA, USA).

Bone densitometry

BMD (g/cm^2) was assessed in anesthetized mice by dual energy X-ray absorptiometry using a PIXImus 2 bone densitometer (GE Medical Systems, Waukesha, WI, USA) as previously described [6]. Left and right femurs and left and right tibias were averaged for each mouse and the means used for group calculations.

Bone histomorphometry

Lumbar vertebrae (L4–L5) from each mouse were dehydrated and embedded in methyl methacrylate. Thin (5 μm) undecalcified bone sections were prepared, and histomorphometric indices were measured in the cancellous bone. Unstained calcein-labelled sections were used for dynamic histomorphometry measurements, and serial sections were stained with VonKossa/MacNeals Tetrachrome for osteoblast measurements. Slides were digitized using a microscope (Olympus IX-70) and digital camera (QIcam) and analysed using image analysis software at 200× or 400× magnification (Bioquant Osteo, Nashville, TN, USA). Mineralizing surface (MS/BS), mineral apposition rate (MAR), bone formation rates (BFR/BS), and osteoblast number (N.Ob) and surface (Ob.S) were quantified according to standard bone histomorphometry procedures and nomenclature [8].

Micro-CT

Micro-CT (μCT) to assess trabecular bone was performed in L3 vertebrae and the distal femoral metaphysis *ex vivo* using a μCT40 scanner (Scanco Medical AG, Brüttisellen, Switzerland) as described [6, 9]. The scanner was calibrated weekly with a factory-supplied phantom. A total of 405 tomographic slices at a voxel size of 6 μm (70 kVp and 114 mA, and with 200 ms integration time) were taken at the L3 vertebra (total area of 2.4 mm), and 100 tomographic slices at the distal femoral metaphysis and trabecular bone segmented from the cortical shell for a total area of 0.6 mm beginning ~0.5 mm from the distal growth plate. Cortical bone was quantified at the femoral mid-diaphysis from 100 tomographic slices (total area of 0.6 mm). Indices and units were standardized as per published guidelines [10].

Biochemical indices of bone turnover

C-terminal telopeptide of collagen type I (CTx) and osteocalcin were quantified in the serum of 2-month-old female C57BL6 mice, treated monthly for 2 months with 10 mg/kg MR1 or isotype control hamster IgG, using RATlaps (CTx) and Rat-MID (osteocalcin) ELISAs (Immunodiagnostic Systems, Fountain Hills, AZ, USA).

Flow cytometry

FoxP3 and CTLA-4 expression were quantified by flow cytometry using antibodies purchased from BioLegend (San Diego, CA, USA). To quantify CTLA-4 and FoxP3 production, splenocytes and whole bone marrow were prepared for intracellular staining using the BioLegend True-Nuclear transcription factor buffer set (BioLegend, San Diego, CA, USA). The cells were permeabilized using the perm buffer from the Tru-Nuclear transcription buffer kit according to the manufacturer's instructions. Intracellular staining was accomplished using anti-mouse CTLA-4 or isotype control antibody (Armenian Hamster IgG-PE) or anti-mouse FoxP3 or isotype control antibody (rat IgG2b, κ-Alexa Fluor 647). Samples were acquired on a BD LSRII Flow Cytometer (BD Immunocytometry Systems, San Jose, CA, USA) and the

data analysed with FlowJo software (Treestar, Ashland, OR, USA). Isotype controls were used to assess non-specific binding for setting gates and fluorescence minus one controls were used to set colour compensation.

APC assays

In vitro APC assays were performed as previously described [6]. Briefly, immunomagnetically purified (Miltenyi Biotech, Auburn, CA, USA) splenic CD11c dendritic cells were isolated from untreated wild-type C57BL6 mice, and used as APCs. APCs were plated in triplicate at 150 000/well in complete RPMI 1640/10% fetal bovine serum and incubated for 4 h at 37°C with 1 μM antigen (ovalbumin peptide) (SIINFEKL; InvivoGen, San Diego, CA, USA), followed by two washes in medium. $CD8^+$ T cells expressing a monoclonal ovalbumin-specific transgenic T cell receptor were immunomagnetically (Miltenyi Biotech, Auburn, CA, USA) purified from the spleens of untreated (Tg) mice expressing a receptor for ovalbumin (OVA) in the context of MHC class I (OT1) mice and pre-incubated with MR1 (10 μg/ml) for 1 h. One million T cells were then incubated for 24 h with ovalbumin-presenting APCs with or without MR1 (5 μg/ml). T cells and dendritic cells were dissolved in TRIzol for RNA isolation and real-time RT-PCR for determination of Wnt-10b expression.

Real-time RT-PCR

Total RNA was extracted in TRIzol reagent. Real-time RT-PCR was performed on an ABI StepOnePlus (Applied Biosystems, Foster City, CA, USA) as previously described [6] using commercial (Applied Biosystems, Foster City, CA, USA) master mix, and primer sets and probes for murine Wnt-10b (Mm00442104**)** and 18 S ribosomal RNA (Mm03928990). Changes were calculated using the $2^{-\Delta\Delta Ct}$ method [11] with normalization to 18 S.

Statistical analysis

Statistical significance was determined using Prizm version 7 for Macintosh (GraphPad Software, La Jolla, CA, USA). Data distributions were assessed using Shapiro–Wilk normality test. Simple comparisons were made using unpaired, two-tailed Student's *t*-test for parametric data or Mann–Whitney test for non-parametric data, as indicated. Multiple comparisons were performed using a one way analysis of variance with Tukey's multiple comparisons *post hoc* test. $P \leqslant 0.05$ was considered statistically significant. All data are presented as mean (S.D.).

Results

BMD is significantly increased in the lumbar spine following MR1 treatment. BMD was quantified by dual energy X-ray absorptiometry at baseline (0 time) and after 6 months of treatment. Data are presented for each anatomic site as BMD (g/cm^2) as well as BMD (percent change from baseline). No significant changes relative to Ig-treated controls were observed for total body (Fig. 1A and B) and long bones, including femurs (Fig. 1E and F) and tibias (Fig. 1G and H). However, lumbar spine BMD was significantly increased relative to control mice (Fig. 1C and D).

MR1 leads to significantly elevated trabecular BV in lumbar vertebrae

Independent structural analysis of the trabecular bone compartment of the lumbar vertebral body was performed using μCT. Representative μCT 3D visual reconstructions of the vertebral trabecular compartment show a consistent increase in bone mass in MR1-treated mice relative to Ig controls (Fig. 2A).

To verify data quantitatively, we calculated microarchitectural indices of vertebral trabecular bone volume (BV) and structure. The data confirmed (Fig. 2D) a significant increase in trabecular BV fraction [BV/tissue volume (TV)] in MR1-treated mice, a consequence of increased BV (Fig. 2C). A small but significant increase in TV was also observed (Fig. 2B). Structural indices revealed that the increase in BV was associated with an increase in trabecular number while trabecular thickness was not significantly changed (Fig. 2E and F, respectively). Increased BV/TV was consistent with a corresponding decline in trabecular separation (Fig. 2G). The index of trabecular volumetric bone density was also significantly increased (Fig. 2H) and the structure model index, a reflection of the rod versus plate-like nature of the trabecular structure, was decreased, suggesting a trend towards a more robust plate-like structure in MR1-treated mice (Fig. 2I).

In contrast to trabecular bone, no significant changes were observed in the cortical compartment of the vertebrae including average cortical thickness, cortical bone area, total cross-sectional area inside the periosteal envelope and the cortical area fraction (Fig. 2J–M, respectively).

In contrast to the axial skeleton, neither femoral cortical nor trabecular compartments showed any significant changes following 6 months of MR1 administration (supplementary Fig. S1, available at *Rheumatology* online).

Taken together our data reveal that MR1 causes a significant gain in vertebral trabecular bone mass in skeletally mature mice, but not in the cortical compartment.

MR1 enhances biochemical indices of bone formation but not indices of bone resorption *in vivo*

After 2 months of treatment with MR1 or Ig no significant difference was observed in the serum marker of bone resorption CTx (Fig. 3A). In contrast, the serum formation marker osteocalcin was significantly increased (Fig. 3B), suggesting that vertebral bone accretion was accounted for by increased bone formation rather than changes in bone resorption.

To assess bone formation at the tissue level, histomorphometry was performed on vertebrae treated for 6 months with MR1 or Ig. Consistent with the μCT outcome, BV/TV was significantly increased by MR1 treatment (Table 1). MS/BS was also significantly increased, but MAR and BFR/BS were not significantly changed. In contrast, Ob.S and N.Ob were both robustly increased by MR1 treatment. Representative calcein double-labelled trabecular bone sections are shown in Fig. 3C.

FIG. 1 BMD is significantly increased in the lumbar spine following MR1 treatment

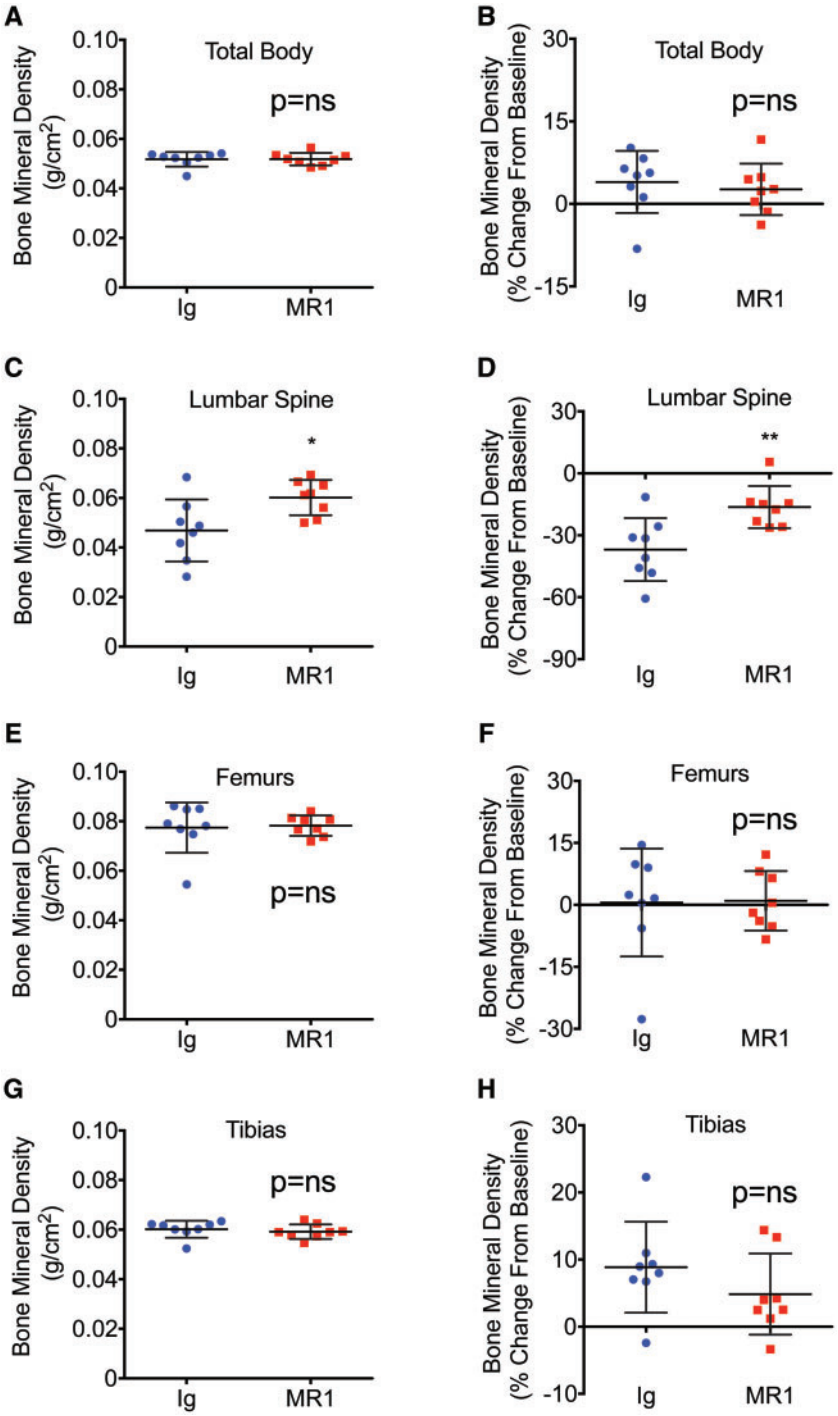

Mice (female C57BL6) were administered Ig (control) or MR1 for 6 months, beginning at 5 months of age. BMD was quantified by DEXA at baseline and at 11 months of age and data are presented as BMD (g/cm^2), as well as BMD (% change from baseline) for total body BMD (**A** and **B**), lumbar spine (**C** and **D**), femur (**E** and **F**) and tibia (**G** and **H**). Mean (S.D.). $^*P < 0.05$; $^{**}P < 0.01$; by Student's *t*-test. $n = 8$ Ig and 8 MR1 mice/group. DEXA: dual energy x-ray absorptiometry; BMD: bone mineral density.

Fig. 2 MR1 promotes trabecular bone accretion in lumbar vertebrae of skeletally mature mice

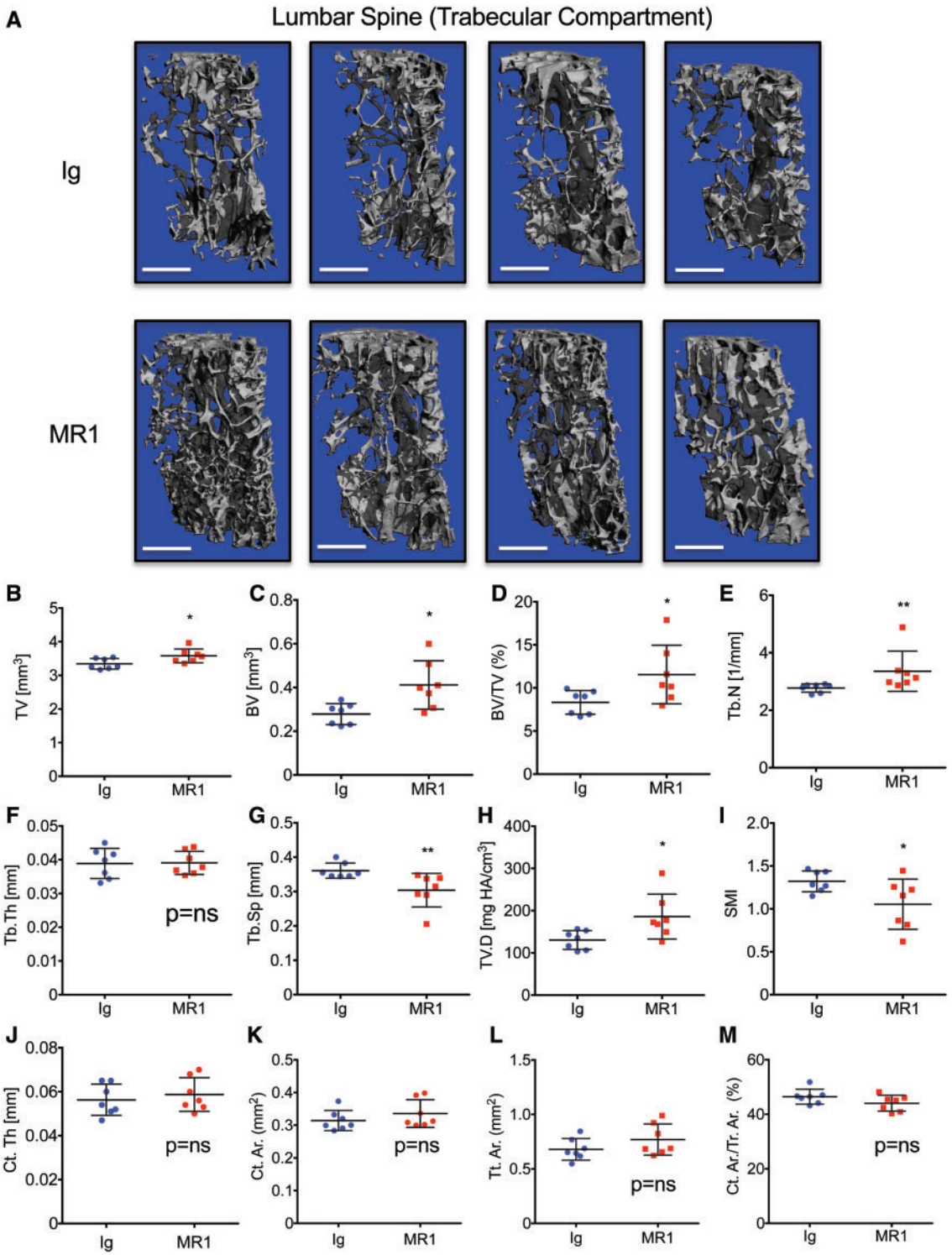

Mice were administered Ig (control) or MR1 for 6 months, beginning at 5 months of age and L3 lumbar vertebrae analysed by micro-CT (μCT). (**A**) Representative μCT reconstructions of trabecular bone. Four representative images are shown for each group. The white scale bar = 500 μm. Quantitative microarchitectural indices of vertebral bone volume and structure were further determined. (**B**) Tissue volume (TV), (**C**) bone volume (BV), (**D**) BV/TV, (**E**) Tb. N, (**F**) Tb.Th, (**G**) Tb.Sp, (**H**) TV.D and (**I**) SMI. Cortical indices: (**J**) Ct.Th, (**K**) cortical bone area (Ct.Ar), (**L**) total cross-sectional area (Tt.Ar) and (**M**) Ct.Ar/Tt.Ar. *$P < 0.05$; **$P < 0.01$; by Mann–Whitney test. $n = 7$ Ig and 7 MR1 mice/group. Mean (S.D.). BV/TV: bone volume fraction; Ct.Th: average cortical thickness; Ct.Ar/Tt.Ar: cortical area fraction; SMI: structure model index; Tb.N: trabecular number; Tb.Th: trabecular thickness; Tb.Sp: trabecular separation; TV.D: trabecular volumetric bone density.

Fig. 3 Biochemical markers of bone formation and quantitative bone histomorphometry in Ig- and MR1-treated mice

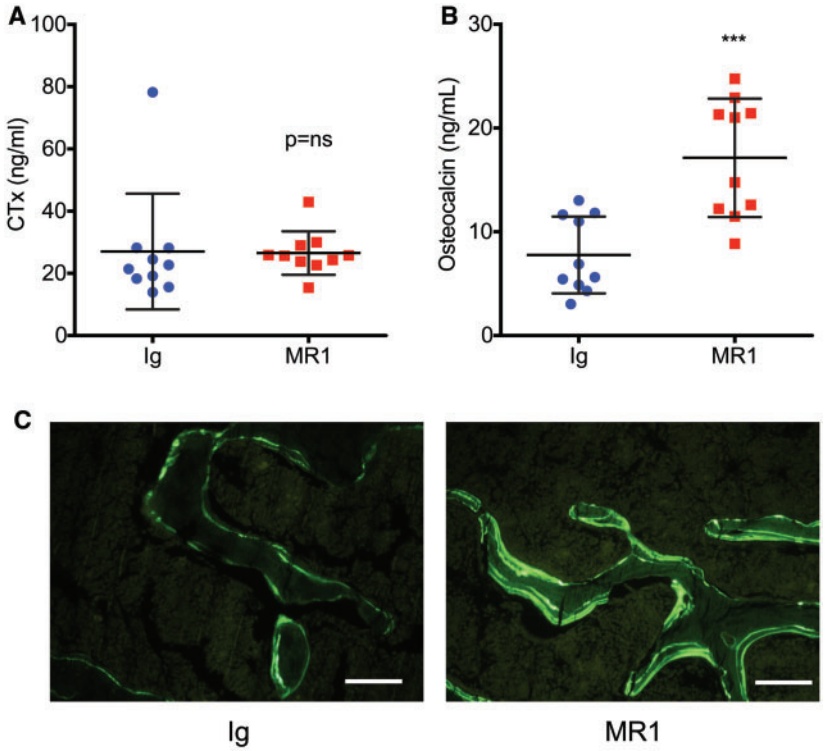

Markers of bone turnover were quantified in serum after administration of MR1 or Ig for 2 months. (**A**) C-terminal telopeptide of collagen type I, a sensitive and specific marker of bone resorption. (**B**) Osteocalcin, a sensitive and specific marker of bone formation. ***$P < 0.001$, by Student's *t*-test, $n = 10$ mice/group. (**C**) Representative images of double calcein labelled vertebral trabecular bone sections from mice treated for 6 months with MR1 or Ig control. White line = 100 micrometers.

Table 1 Bone histomorphometry of vertebrae treated with MR1 or Ig for 6 months

Index	Ig	MR1	% Change	*P*-value
BV/TV, mean (S.D.), %	0.0861 (0.0278)	0.1777 (0.0532)	+106.3	0.0017
MS/BS, mean (S.D.), %	0.2833 (0.0819)	0.3902 (0.0528)	+37.7	0.0133
MAR, mean (S.D.), μm/day	1.0742 (0.2195)	0.9623 (0.1230)	−10.4	0.2617
BFR/BS, mean (S.D.), μm/day	0.3163 (0.0931)	0.3795 (0.0924)	+20.0	0.2990
N.Ob/BS, mean (S.D.), mm	4.67 (2.49)	14.29 (2.69)	+205.7	<0.0001
Ob.S/BS, mean (S.D.), %	8.55 (8.50)	25.82 (6.52)	+201.7	<0.0001

All values listed as mean (S.D.). $N = 7$ samples/group. *P*-value: actual *P*-values by Student's *t*-test; BS: bone surface; BV/TV: bone volume fraction; MS: mineralizing surface; MAR: mineral apposition rate; BFR: bone formation rate; Ob.S: osteoblast surface; N.Ob: number of osteoblasts.

MR1 induces Wnt-10b production by T cells *in vivo*, in a major histocompatibility complex I (MHCI) APC assay *in vitro*, and induces Treg formation and CTLA-4 production *in vivo*. To investigate the bone anabolic effect of MR1, we purified splenic T cells from mice treated with MR1 or Ig for 2 months and performed real-time RT-PCR quantification of Wnt-10b, a bone anabolic ligand. MR1 induced a significant increase in Wnt-10b mRNA (Fig. 4A).

Using an *in vitro* APC assay we further found that $CD8^+$ T cells alone expressed only low basal levels of Wnt-10b mRNA, while Wnt-10b from APC alone was not detected. Coculture of APC with $CD8^+$ T cells however, led to a significant induction of Wnt-10b, which was further significantly increased by addition of MR1 (Fig. 4B).

Flow cytometric analysis revealed that CTLA-4, an inducer of Wnt-10b, was significantly increased in splenic lymphocytes (Fig. 4C) and nucleated bone marrow cells (Fig. 4D) isolated from mice treated for 2 months with MR1 (Fig. 4B).

Finally, as MR1 has been previously reported to stimulate formation of Tregs [12], a population that secretes high levels of CTLA-4, we analysed by flow cytometry

Fig. 4 MR1 induces Wnt-10b production by T cells in an antigen-presenting cell assay and promotes Treg formation and cytotoxic T lymphocyte antigen 4 production

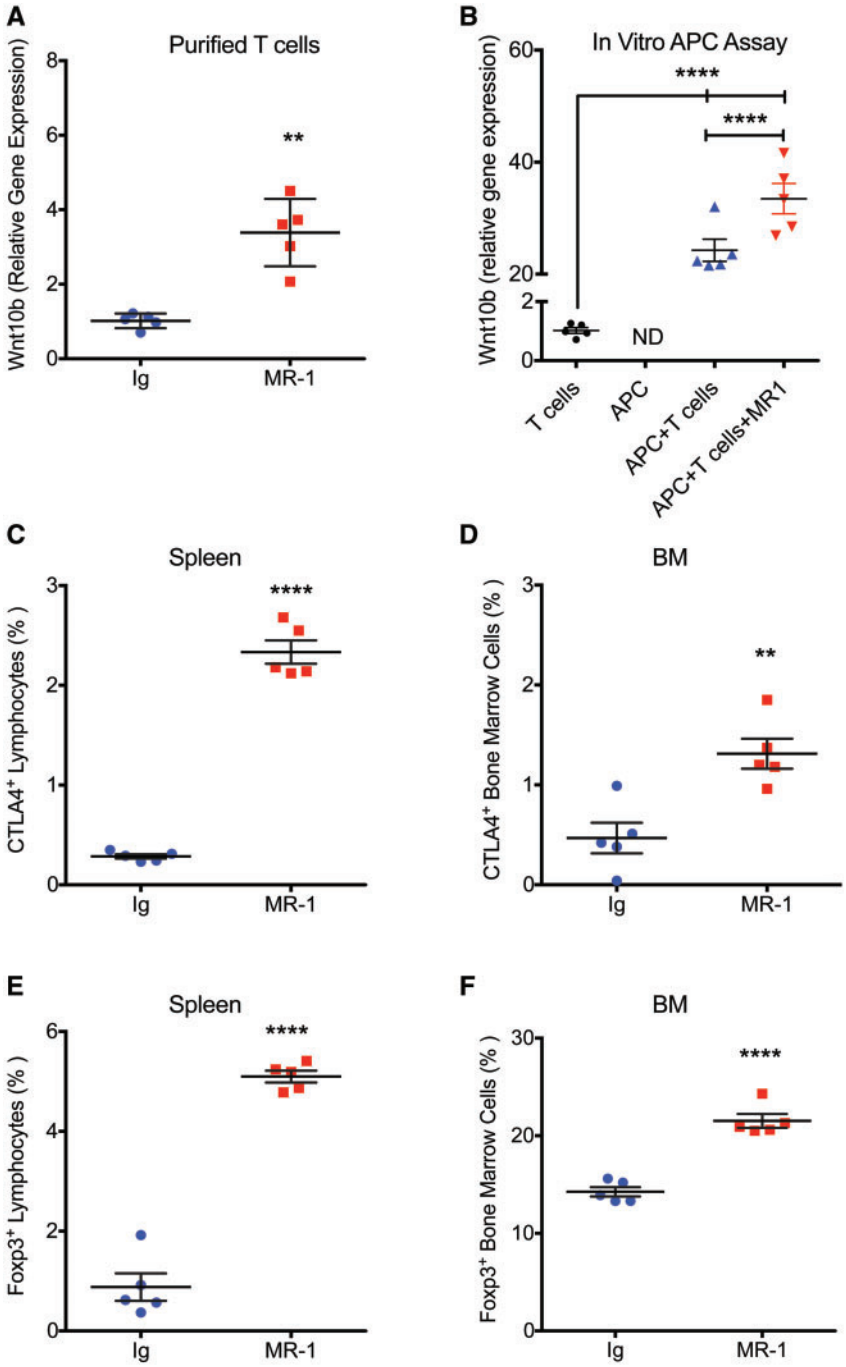

(**A**) Mice were treated with MR1 for 2 months and Wnt-10b was quantified by real-time RT-PCR in immunomagnetically purified splenic T cells. $^{**}P < 0.01$ by Mann–Whitney test. (**B**) MHCI antigen-presenting cell (APC) assay followed by RT-PCR quantification of Wnt-10b production by $CD8^+$ T cells alone (control), APC alone, $CD8^+$ T cells co-cultured with ovalbumin expressing APC, treated with or without MR1 (5 μg/ml). $n = 5$ independent wells/group. $^{****}P < 0.0001$; by one-way analysis of variance with Tukey's Multiple Comparison post-test. ND: not detected. (**C**) Cytotoxic T lymphocyte antigen 4 (CTLA-4) expression in spleen and (**D**) bone marrow (BM) by flow cytometry. (**E**) FoxP3 expression in spleen and (**F**) BM by flow cytometry. $^{**}P < 0.01$; $^{****}P < 0.0001$; Student's *t*-test. $n = 5$ mice/group. All data are presented as mean (S.D.). BM: bone marrow; MHCI: major histocompatibility complex I; RT-PCR: reverse transcription polymerase chain reaction.

splenic lymphocytes and nucleated bone marrow cells for FoxP3 expression. Our data document a significant increase in splenic lymphocytes and bone marrow cells expressing FoxP3 (Fig. 4E and F).

Taken together, our data support a model in which MR1 promotes formation of Tregs secreting CTLA-4, which renders T cells anergic, leading to Wnt-10b production and bone anabolism.

Discussion

Anti-CD40L antibodies are in development for amelioration of inflammatory diseases; however, in this study we assessed MR1 activity in the context of healthy wild-type mice. Our data suggest that acute CD40L suppression in this context is bone anabolic, with no change in bone resorption marker being observed.

Histomorphometric analyses confirmed an increase in BV/TV and mineralizing surface and identified a robust increase in osteoblast number and surface. These data suggest a significant increase in osteoblast formation and/or longevity following MR1 treatment; however, activity per osteoblast was likely not increased given that MAR and BFR/BS were not significantly changed.

Bone accretion required several months to achieve a statistically significant increase in BMD. The slow kinetics are likely explained by the relatively low number of activated T cells present under physiological conditions that are capable of being rendered anergic. These activated T cells are likely associated with basal immune surveillance and reactivity to environmental antigens such as gut microbiota [13], and immune renewal functions involving low-affinity interactions with self-peptides [14]. However, in the context of an inflammatory state such as RA, CD40L neutralization is likely to mediate a more complex action on bone turnover. We speculate that MR1 could function not only as a bone anabolic agent but also as an anti-inflammatory, breaking the cycle of T cell activation and blunting inflammatory cascades. This would lead to a relatively diminished osteoclastogenic bone resorption and a slowing of bone loss. In addition, with increased concentrations of activated T cells present in inflammatory states that are available for anti-CD40L treatment to render anergic, a more potent enhancement of bone anabolism than we presently observed under physiological conditions is possible.

Our previous report of genetic ablation of CD40 or CD40L in mice [15], and the report of defective CD40L in humans with X-linked hyper-IgM syndrome [16], both caused a net osteopenic phenotype, while acute pharmacological suppression of CD40L costimulation by MR1 led to a bone anabolic phenotype. One possible explanation for this difference is that chronic lack of CD40L costimulation during development of the immune system may lead to a damaged and dysfunctional adaptive immune response prone to large numbers of defective B cells characterized by diminished osteoprotegerin (OPG) production. In contrast, pharmacological suppression of CD40L in an otherwise intact and mature immune system may predispose T cells towards anergy and hence Wnt-10b production.

As CD40L is upregulated on activated T cells, which represent a relatively small population in healthy organisms, the MR1 target population is likely small and normal B cell homeostasis and OPG production may thus continue largely unaffected. Altering the B cell OPG ratio does however, occur under conditions of more robust immune alteration, such as in HIV infection. We have shown that damage to $CD4^+$ T cells in the HIV-transgenic rat model does indeed promote a decline in B cell OPG, as well as an increase in B cell receptor activator of NF-κB ligand (RANKL), which together skew the RANKL/OPG ratio in favour of bone resorption and loss [17]. This effect was also documented in humans infected with HIV, where the B cell RANKL/OPG ratio correlated significantly with loss of BMD in the appendicular skeleton [18].

We have previously reported that T cells rendered anergic by treatment with CTLA-4Ig (abatacept), a pharmacological CD28 costimulation inhibitor, secrete the bone anabolic factor Wnt-10b [6]. Furthermore, T cells treated with intermittent PTH likewise secrete Wnt-10b, which is permissive and necessary for the full anabolic effects of PTH [5]. Because CD40L blockade has been reported to promote T cell anergy [7], we further investigated whether the bone anabolic activity was also associated with anergic T cells and production of Wnt-10b following CD40L neutralization. Indeed, purified T cells from MR1-treated mice did indeed express higher concentrations of Wnt-10b mRNA, supporting this putative mechanism. This was further supported by our *in vitro* APC assay demonstrating the capacity of MR1 to promote Wnt-10b expression in cultures of APC-activated $CD8^+$ T cells. Furthermore, in our previous studies Wnt-10b production was induced by CTLA-4Ig-induced T cell anergy in mice [6]. In the current studies, we thus examined whether MR1 may promote the production of CTLA-4Ig's physiological counterpart, CTLA-4. CTLA-4 is a factor secreted by B cells, activated $CD8^+$ and $CD4^+$ T cells, and by Tregs [19]. Our data do indeed support a significant increase in CTLA-4 expression in bone marrow and spleen, suggesting a mechanism whereby MR1 induced production of CTLA-4.

Tregs are a population of immunosuppressive T cells, derived mainly from $CD4^+$ T cells, although in the context of skeletal regulation, $CD8^+$ Tregs have been reported to be induced through APC activity with osteoclasts, acting as a negative feedback loop to limit bone resorption in mice [20]. $CD8^+$ Tregs may also mediate direct bone anabolic activity through production of low-dose RANKL [21]. A key mechanism by which Tregs promote immune tolerance is through CTLA-4 production. Consequently, we further tested the capacity of MR1 to promote an increase in Tregs *in vivo*. Our data confirmed a significant increase in bone marrow and spleen lymphocytic FoxP3, a transcription factor diagnostic of Tregs, supporting the conclusion that MR1 promotes Treg formation.

Taken together our data support a model whereby CD40L neutralization by MR1 of both activated $CD4^+$ and $CD8^+$ T cells, promotes CTLA-4 production as well as Treg formation by $CD4^+$ T cells, a significant additional source of CTLA-4. CTLA-4 disrupts the critical CD28

Fig. 5 Model of MR1-induced bone anabolism

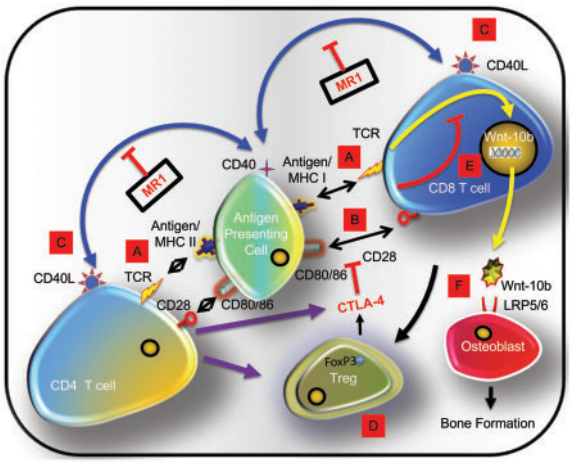

(**A**) Immune responses initiated by engagement of APC expressing antigen as part of MHCI ($CD8^+$ T cells) or MHCII ($CD4^+$ T cells). (**B**) A costimulatory signal is necessary for T cell activation and provided by T cell CD28 binding to APC CD80/86. (**C**) CD40L on activated T cells associates with APC CD40. (**D**) MR1 blocks CD40/CD40L costimulation causing differentiation of $FoxP3^+$ Tregs and cytotoxic T lymphocyte antigen 4 (CTLA-4) secretion disrupting CD28 costimulation causing T cell anergy. (**E**) Anergic $CD8^+$ T cells produce Wnt-10b, a bone anabolic factor. (**F**) Wnt-10b binds to receptors (LRP5/6) on osteoblast lineage cells, promoting bone formation. APC: antigen presenting cell; MHC: major histocompatibility complex.

costimulatory signal on both $CD4^+$ and $CD8^+$ T cells that is necessary for T cell activation, and renders these cells anergic. Anergic $CD8^+$ T cells produce Wnt-10b that binds to the Wnt receptors (LRP5/6) on osteoblast lineage cells, promoting bone formation (Fig. 5).

CD40 signalling has been reported to potentiate the bone anabolic activity of intermittent PTH treatment through direct effects on osteoblasts [22]. CD40L neutralization might thus be expected to suppress osteoblast activity in our study rather than promote it. Given this outcome it appears that the bone anabolic activity of Wnt-10b, secreted by anergic T cells, is able to overcome any detrimental effects of CD40L loss on osteoblast lineage cells. It is possible, however, that the anabolic response would be even more robust if osteoblast CD40 activation were not impeded.

The reason for the bone anabolic effect being limited to the vertebrae is unclear, but one possible explanation is that bone formation was most pronounced in the trabecular bone compartment, and the vertebral body is enriched in this type of bone compared with long bones. We used mice 5 months of age with a mature skeleton, and there is very little trabecular bone template in the femoral metaphasis at this age compared with young immature animals. The vertebral body by contrast is still a rich source of trabecular bone and may have provided sufficient template for osteoblasts to act on. The apparent specificity of MR1-induced anabolism for trabecular bone may relate to the relatively low anabolic activity that is sufficient over time to modulate the trabecular compartment, which is more metabolically active, but is of insufficient magnitude to significantly increase cortical bone in over the experimental time frame.

Given that biochemical makers reflect global bone turnover and hence predominantly cortical bone, the relatively large increase in serum osteocalcin, quantified at 2 months of treatment, suggests that MR1 action may have indeed involved both bone compartments initially, with cortical apposition dwindling shortly after attainment of peak BMD, when basal bone formation and cortical apposition slows significantly.

The net effect of CD40L neutralization on the human skeleton is presently unknown and in fact, direct targeting of CD40L in humans was not found to be a viable therapeutic strategy in clinical trials owing to cross-reactivity with platelets that creates a potential for thromboembolic complications and a poor harm/benefit ratio. However, blockade of the CD40/CD40L pathway remains a highly effective method for inducing transplantation tolerance and interest remains in developing alternative methods of inhibiting CD40/CD40L [23]. Recent studies in nonhuman primates show that Fc-silent anti-CD40 monoclonal antibodies are indeed capable of prolonging renal allograft survival in the absence of thromboembolism [24] and consequently this costimulatory pathway remains a viable putative target. One future application of CD40/CD40L suppression suggested by our study is to stimulate new bone formation to promote trabecular bone regeneration in the vertebrae. However, a potential for increased osteoclastogensis causing skeletal damage remains a possible outcome under certain conditions and will need to be carefully studied in the relevant patient population(s) involved.

Conclusion

In conclusion, our data demonstrate the complexity of the immuno-skeletal interface and the context dependency of outcomes based on costimulatory manipulation with the capacity to lead to either bone resorption or bone formation. The effects of immunomodulatory agents in humans may be even more complex and difficult to predict, and certainly caution is needed regarding side-effects of such agents on the skeleton. However, under appropriate conditions, CD40L suppression may promote Wnt-10b production and a bone anabolic response with beneficial net gain in trabecular bone mass in the axial skeleton.

Acknowledgements

The authors thank Dr Daiana Weiss (Emory University) for critical reading of the manuscript and Ms Penny Roon and the Augusta University Electron Microscopy and Histology Core Laboratory for preparation of histological sections for histomorphometry. Authors' contributions: M.N.W. conceived the study, performed data analysis and drafted the manuscript. S.R.-P., T.V., M.E.M.-L. and K.Y. performed data acquisition, data analysis and revised and

finalized the manuscript. All authors read and approved the final manuscript and gave consent for publication in the journal *Rheumatology*. M.N.W. was also supported, in part, by grants from the National Institutes of Health including the National Institute of Arthritis and Musculoskeletal and Skin Diseases (grant numbers AR056090, AR059364, AR068157 and AR070091) and the National Institute on Aging (grant number AG040013). M.E.M.-L. was supported by the National Institute on Aging (AG036675).

Funding: This work was supported by a grant from the Biomedical Laboratory Research & Development (BLRD) Service of the VA Office of Research and Development (5I01BX000105) to M.N.W. The contents of this manuscript do not represent the views of the Department of Veterans Affairs.

Disclosure statement: The authors have declared no conflicts of interest.

Supplementary data

Supplementary data are available at *Rheumatology* online.

References

1 Daoussis D, Andonopoulos AP, Liossis SN. Targeting CD40L: a promising therapeutic approach. Clin Diagn Lab Immunol 2004;11:635–41.

2 Dejica DI, Manea EM. Costimulatory molecule CD154 in systemic lupus erythematosus and rheumatoid arthritis. Therapeutic perspectives. Roum Arch Microbiol Immunol 2006;65:66–74.

3 Grewal IS, Flavell RA. The CD40 ligand. At the center of the immune universe? Immunol Res 1997;16:59–70.

4 Homig-Holzel C, Hojer C, Rastelli J *et al*. Constitutive CD40 signaling in B cells selectively activates the noncanonical NF-kappaB pathway and promotes lymphomagenesis. J Exp Med 2008;205:1317–29.

5 Terauchi M, Li JY, Bedi B *et al*. T lymphocytes amplify the anabolic activity of parathyroid hormone through Wnt10b signaling. Cell Metab 2009;10:229–40.

6 Roser-Page S, Vikulina T, Zayzafoon M, Weitzmann MN. CTLA-4Ig-induced T cell anergy promotes Wnt-10b production and bone formation in a mouse model. Arthritis Rheumatol 2014;66:990–9.

7 Quezada SA, Fuller B, Jarvinen LZ *et al*. Mechanisms of donor-specific transfusion tolerance: preemptive induction of clonal T-cell exhaustion via indirect presentation. Blood 2003;102:1920–6.

8 Dempster DW, Compston JE, Drezner MK *et al*. Standardized nomenclature, symbols, and units for bone histomorphometry: A 2012 update of the report of the ASBMR Histomorphometry Nomenclature Committee. J Bone Miner Res 2013;28:2–17.

9 Ofotokun I, Titanji K, Vikulina T *et al*. Role of T-cell reconstitution in HIV-1 antiretroviral therapy-induced bone loss. Nat Commun 2015;6:8282.

10 Bouxsein ML, Boyd SK, Christiansen BA *et al*. Guidelines for assessment of bone microstructure in rodents using micro-computed tomography. J Bone Miner Res 2010;25:1468–86.

11 Livak KJ, Schmittgen TD. Analysis of relative gene expression data using real-time quantitative PCR and the 2(-Delta Delta C(T)) method. Methods 2001;25:402–8.

12 Vogel I, Verbinnen B, Van Gool S, Ceuppens JL. Regulatory T cell-dependent and -independent mechanisms of immune suppression by CD28/B7 and CD40/CD40L costimulation blockade. J Immunol 2016;197:533–40.

13 Sjogren K, Engdahl C, Henning P *et al*. The gut microbiota regulates bone mass in mice. J Bone Miner Res 2012;27:1357–67.

14 Surh CD, Sprent J. Homeostatic T cell proliferation: how far can T cells be activated to self-ligands? J Exp Med 2000;192:F9–14.

15 Li Y, Toraldo G, Li A *et al*. B cells and T cells are critical for the preservation of bone homeostasis and attainment of peak bone mass in vivo. Blood 2007;109:3839–48.

16 Lopez-Granados E, Temmerman ST, Wu L *et al*. Osteopenia in X-linked hyper-IgM syndrome reveals a regulatory role for CD40 ligand in osteoclastogenesis. Proc Natl Acad Sci USA 2007;104:5056–61.

17 Vikulina T, Fan X, Yamaguchi M *et al*. Alterations in the immuno-skeletal interface drive bone destruction in HIV-1 transgenic rats. Proc Natl Acad Sci USA 2010;107:13848–53.

18 Titanji K, Vunnava A, Sheth AN *et al*. Dysregulated B cell expression of RANKL and OPG correlates with loss of bone mineral density in HIV infection. PLoS Pathog 2014;10:e1004497.

19 McCoy KD, Le Gros G. The role of CTLA-4 in the regulation of T cell immune responses. Immunol Cell Biol 1999;77:1–10.

20 Buchwald ZS, Kiesel JR, Yang C *et al*. Osteoclast-induced Foxp3+ CD8 T-cells limit bone loss in mice. Bone 2013;56:163–73.

21 Buchwald ZS, Yang C, Nellore S *et al*. A bone anabolic effect of RANKL in a murine model of osteoporosis mediated through FoxP3+ CD8 T cells. J Bone Miner Res 2015;30:1508–22.

22 Robinson JW, Li JY, Walker LD *et al*. T cell-expressed CD40L potentiates the bone anabolic activity of intermittent PTH treatment. J Bone Miner Res 2015;30:695–705.

23 Ferrer IR, Wagener ME, Song M *et al*. Antigen-specific induced Foxp3+ regulatory T cells are generated following CD40/CD154 blockade. Proc Natl Acad Sci USA 2011;108:20701–6.

24 Cordoba F, Wieczorek G, Audet M *et al*. A novel, blocking, Fc-silent anti-CD40 monoclonal antibody prolongs nonhuman primate renal allograft survival in the absence of B cell depletion. Am J Transplant 2015;15:2825–36.